Studies on the Morphological Changes by Numerical Modeling Along Kakinada Coasts

N. Sharmila, R. Venkatachalapathy and M. Mugilarasan

Abstract Prediction of morphological changes has immense application for development of coastal infrastructure. More relevantly, various sectors are facing the coastal erosion problem, which needs to develop the model for the concern coasts. Even though there are a number of free softwares available to model and validate the coast, commercially available softwares such as MIKE 21 were used in the present study. Hence, this chapter investigates the hydrodynamics, spectral waves and sediment transport modeling by dynamic coupling of waves and currents using MIKE 21 Flexible Mesh coupled model at Kakinada coast. For this study, waves, tides and current data were collected during July and December 2009 (NE and SW seasons). Further, the simulation was done by preparing the model, evaluating the critical factor and providing the sensitivity analysis to evaluate the sediment transport pattern at Kakinada coast. Finally, the model performs various statistical measures and were compared with observed data for calibration during SW and NE monsoons. This calibration shows that the observed data has good agreement with model data. Hence, the overall simulation shows that the transport of sediment is strongly controlled by tidal currents and wave ordination, which significantly enhances bed shear stress that results in increases of sediment remobilization.

Keywords MIKE 21 · Tidal currents · Sediment transport · Morphological Hydrodynamics · Spectral waves

N. Sharmila (✉)
International Maritime Academy, Jamin Kottur, Puduchatram, Chennai 600124, Tamil Nadu, India
e-mail: sharmila1512@gmail.com

R. Venkatachalapathy
Faculty of Marine Sciences, Centre of Advanced Study in Marine Biology, Annamalai University, Parangipettai 608502, Tamil Nadu, India

M. Mugilarasan
NCSCM, Anna University, Chennai, Tamil Nadu, India

K. Murali et al. (eds.), *Proceedings of the Fourth International Conference in Ocean Engineering (ICOE2018)*, Lecture Notes in Civil Engineering 23,
https://doi.org/10.1007/978-981-13-3134-3_10

1 Introduction

Coastal morphodynamics provide a key role in understanding the interaction of forces and topography that give rise to the distinctive characters of the world's shoreline. Morphological models are based on the empirical field and laboratory studies, supplemented by computer simulations which helps to generate a greater understanding of coastal regions [1]. Computer simulation can be based on the pattern of change inferred over long timescales and consistent with a process known to operate over shorter timescales. The coastal morphodynamics is concerned primarily with physical features and environmental in the coastal regions, which occurs over a broad range of time and length scale. Sambasiva Rao and Vaidyanadhan [2, 3], Sastry et al. [4], Rengamannar and Pradhan [5] had made deliberate morphological changes around the Godavari delta region. Later, Ramkumar [6, 7] had made an attempt to study morphological evolution off Kakinada bay. Several researchers had studied about sediment characteristics [8–11] using transport along shore flow pattern [12] and multi-data satellite sensor data [13, 14] with GIS technique [15–18]. Guru Prasad and Gaddem [19] had presented about the global warming effects on Uppada coast, a fishing village of Andhra Pradesh. Nageswara Rao et al. [20, 21] had studied the Holocene evolution and coastal morphodynamics of Godavari estuary. Satyaprasad [22] studied about the morphodynamics of the beaches and sand spit, Kakinada Bay. Recently, Jain et al. [23] studied on Morphodynamics of Godavari Tidal Inlets and Kakinada spit using time series multi-sensor satellite data for the period of 1987–2004. No such systematic approach had been made to study the Kakinada coast using modeling software.

The primary aim of this chapter is to simulate hydrodynamic, spectral wave, and sediment transport modeling using dynamic coupling of waves and currents. The objectives are to understand the hydrodynamic and sediment transport of the study area; prepare a model to represent the hydrodynamic conditions at the locations using MIKE 21 FM coupled model and evaluating the sediment transport pattern in that location; identify the critical factor in hydrodynamic, spectral and sediment transport modeling in the study area and provide a sensitivity analysis for the parameter governing sediment transport and finally assess the performance of the model using statistical tools and techniques have been made by comparing the model-derived parameters against the corresponding observed data.

2 Study Area

Kakinada (long. 82° 14′–82° 22′ E and lat. 16° 5′–17° 05′) is situated on the east coast of India, about 160 km southwest of Visakhapatnam. It has an average elevation of 2 m (6 ft) from mean sea level. It is the main receptacle for the river run into the Godavari estuarine system. The total area of the bay is 132 km^2, which contribute two major distributors of the river Godavari which are Coringa and Gaderu opening into the

Kakinada bay. River Godavari transports a considerable quantity of sediments to the sea, which nourishes the sandy beaches in the vicinity. The Seafloor up to a distance of 3 km is sand, from 3 to 20 km it is covered with clay, and up to 20–30 km, it is covered with shells the outermost zone consisting of clay, fine sand, and shell fragments [8]. The geomorphology of the Kakinada coast consists of mudflats, mangrove swamps, sandy beach, and sandy Island. On the western side of Kakinada coast is the mainland of Kakinada which was formed by deltaic and flood plains. The coastal strip north of Kakinada consists of windblown sand and sand dunes which are succeeded landward by laterites, sandstones and Khondalities. The lowest part of the delta is made of a series of sand ridges interpreted to be ancient beach ridge forms, due to high waves and detrital materials brought by the river from its drainage basin. On the eastern side of the bay, there is a long narrow sandbar continuous with the eastern tip of the Hope Island separating the bay from the sea. Due to the presence of the sandbar, the Kakinada bay forms a semi-enclosed body of water where the water movements are unique. An industrial belt, running north–south the length of the city, separates the eastern part of the coast. Uppada beach is primarily considered as Kakinada beach which has one of the longest coastlines in Indian beaches.

3 Methodology

3.1 Field Investigation

The bathymetry survey was carried out in the Kakinada coast from north of Godavari to Uppada including bay region, during July 2009 using single beam echo-sounder (ODOM Hydrotrac) interfaced to a differential global positioning system (DGPS-Trimble) and laptop computer in a water-resistant case mounted on a fishing trawler boat along with heave sensor (HS-50, Heave sensor). Wave and tide parameters were measured using the MIDAS Wave Recorder (Valeport tide gauges—Valeport Limited, U.K.) and current data was measured using Recording Current Meters (Aanderaa RCM9) for two monsoons (northeast (NE) and southwest (SW) monsoon) from 14 to 28 July and 14 to 30 December during 2009 at Kakinada coast, respectively (Table 1).

3.2 Numerical Model

In this chapter MIKE 21/3 Coupled FM module (integration of Mike 21 HD, SW and ST modules) developed by DHI by combined wave/current/sediment transport for the study area. The reason for selection of MIKE 21/3 Coupled FM models is that they suit for the condition of flexible mesh, which enables more accurate representation and easy user interface to handle the problems with better real-time scenario. The flexible mesh also allows reducing the grid size locally at areas of special interest.

Table 1 Deployment locations for Kakinada coast

Location no.	Location name	Latitude (°N)	Longitude (°E)	Deployment depth (m)	Instrument name	Tide measuring interval (min)
1	Offshore	17° 02.154′	82° 24.181′	19.5	Valeport 730D and Aanderaa-RCM9	12
2	Mouth of bay	17° 05.589′	82° 25.698′	8.1	Valeport 730D and Aanderaa-RCM9	12
3	Near Godavari	16° 49.885′	82° 24.111′	8.1	Valeport 730D and Aanderaa-RCM9	12

Coupled FM model simulates three models in parallel while interchanging the input of one model to simulate the output of another model. Wave radiation stress obtained as the SW model output is fed input to the hydrodynamic model. Water level flow and current variation from HD model provides input to the ST model.

3.3 Model Setup

3.3.1 Bathymetry

Setting up a mesh includes appropriate selection of the area to be modeled, adequate resolution of the bathymetry, flow, wind and wave fields under consideration and definition of codes for open and land boundaries. The model is set up as a UTM-44 projection using depth data from nearshore surveyed bathymetry data. The model computational domain (520 km^2) has 20×26 km in x and y directions, respectively. A nested approach is used to create the mesh for minimizing the errors in calculation of results. The large and small mesh was created, for which larger domain a resolution of 7 km is used progressively reducing to 12 km for Kakinada coast. The total number of elements used in this mesh is 6232 with 3600 nodes. To run the model, stability used here as The Courant–Friedrichs–Lewy (CFL) number which is chosen as 0.9.

3.3.2 Hydrodynamic Model

The hydrodynamic module is based on the numerical solution of the two-dimensional shallow water equation the depth-integrated incompressible Reynolds averaged Naviers–Stokes equation. Thus, the model consists of continuity, momentum, temperature, salinity, and density equations.

The following equations are used to obtain the conservation of mass and momentum integrated over the vertical flow and water-level variation.

$$\frac{\partial \zeta}{\partial t} + \frac{\partial p}{\partial x} + \frac{\partial q}{\partial y} = \frac{\partial d}{\partial t}$$

$$\frac{\partial p}{\partial t} + \frac{\partial}{\partial x}\left(\frac{p^2}{h}\right) + \frac{\partial}{\partial y}\left(\frac{pq}{h}\right) + gh\frac{\partial \zeta}{\partial x} + \frac{gp\sqrt{p^2+q^2}}{c^2 \cdot h^2} - \frac{1}{\rho_w}\left[\frac{\partial}{\partial y}(h\tau_{xx}) + \frac{\partial}{\partial y}(h\tau_{xy})\right] - \Omega_q - fVV_x + \frac{h}{\rho_w}\frac{\partial}{\partial_x}(p_a) = 0$$

$$\frac{\partial q}{\partial t} + \frac{\partial}{\partial y}\left(\frac{q^2}{h}\right) + \frac{\partial}{\partial x}\left(\frac{pq}{h}\right) + gh\frac{\partial \zeta}{\partial y} + \frac{gp\sqrt{p^2+q^2}}{c^2 \cdot h^2} - \frac{1}{\rho_w}\left[\frac{\partial}{\partial y}(h\tau_{yy}) + \frac{\partial}{\partial x}(h\tau_{xy})\right] - \Omega_p - fVV_y + \frac{h}{\rho_w}\frac{\partial}{\partial_{xy}}(p_a) = 0$$

Various sensitivity tests were carried out to analyze the effect of variations of different parameters on the hydrodynamic model results. Flooding depth was set at 0.05 m, and drying depth was set at 0.15 m to capture the intertidal area appropriately in the model domain. Bed resistance was calculated using the roughness heights as Chezy number of 72 m^3/s. Horizontal eddy viscosity coefficient defines as the turbulent mixing in the water in which Smagorinsky eddy viscosity with the coefficient of 0.5 was adopted for the simulation. The wind shear stress was simply assumed to be proportional to square of wind velocity through using the wind drag coefficient. The drag coefficient depends on the wind speed and increased with the increase of wind speed. Comparing the outputs with measurements, the drag coefficient of 0.001255 (for wind speed of 7 m/s) and 0.0026 (for wind speed of 15 m/s and higher) was chosen. The numerical simulations were carried out by imposing two open boundaries, viz., north and south of Kakinada port and the offshore boundary was considered to be zero cross flow. The model was driven by temporal variations in water level specified along the open boundaries and wind, to obtain realistic water elevation and flow patterns.

3.3.3 Spectral Wave Model

The discretization in geographical and spectral space is modeled using a cell-centered finite volume method. In the geographical domain, an unstructured mesh is used as base model. The integration time is based on a fractional step approach [24].

In Cartesian coordinates, the conservation for the wave action can be written as

$$\frac{\partial N}{\partial t} + \nabla.(\vec{v}N) = \frac{s}{\sigma}$$

where N ($\vec{x}$, σ, θ, t) is the action density, t is the time, $\vec{x} = (x, y)$ is the Cartesian coordinates, $\vec{v} = (C_x, C_y, C_\sigma, C_\theta)$ is the propagation velocity of the wave group in the four-dimensional phase space $\vec{x}$, y, σ, and θ, and S is the source term for the energy balance equation ∇ is the four-dimensional differential operator in the $\vec{x}$, y, σ, θ-space.

The sensitivity analysis for the present study, the optimum values of wave breaking parameter ($\gamma = 0.8$), bottom friction (Nikuradse roughness) ($K_n = 0.04$ m), and white capping coefficients ($C_{dis} = 4.5$) was used in the fully spectral experiment. The wave spectrum was represented by 16 discrete directions and 25 discrete frequency bins logarithmically spaced from 0.055 to 0.6 Hz. In this formulation dissipation coefficient depended on wave hydrodynamic conditions. This dissipation coefficient also was used as a tuning parameter in which white capping dissipation source function included two free parameters; C_{dis} and $DELTA_{dis}$ [25]. In this present model, C_{dis} coefficient was given as 4.5 and $DELTA_{dis}$ as 0.5. The model was given as a cold start and spun up. The initial conditions were calculated by the model from the first time step of the wind field, using JONSWAP fetch growth expressions. These wave parameters were input at the offshore boundary, on the north and south boundary the MIKE 21 option "lateral boundary" was used whereby the basic equations were calculated along the boundary line by taking the offshore end and reducing to zero at the inshore end.

3.3.4 Sediment Transport

In the near shore region, the analysis of the erosion–accretion plays an vital importance for the development of a harbor and construction of coastal structures. MIKE 21/3 Coupled Flow Model—ST describes erosion, transport, and deposition of sand under the action of pure current or under wave and currents [26]. The sediment transport rates are calculated using two different model types; "Pure Currents" and "Combined Currents and Waves". For "Pure Currents", the rates are calculated directly on the actual conditions. For "Combined Currents and Waves," the rates are found by linear interpolation of transport in sediment transport table. In the present study, sediment transport rates are simulated using Combined Waves and Current model, in which sediment transport model (STPQ3D) is prepared. Sediment transport also depends upon the nature of seabed and its grain size distribution. For which, the

sediment properties like porosity and grain diameter were taken from the reference values reported by Narasiman et al. [27] (porosity as 0.4, grain diameter as 0.2 mm and grading coefficient is selected as 1.1). Before commencing the modeling, a sediment transport table is needed to be generated with the help of MIKE 21 toolbox. Bank erosion effect is included as 30° for the ST simulating model. The forcing parameters (waves, water flow, and current variation) are incorporated from hydrodynamics and spectral wave model in ST model for creating a sediment transport model which includes the dynamic of both waves and currents. For ST simulation boundary conditions, "Zero sediment flux gradient for outflow, zero bed change for inflow" was selected for all three boundaries (offshore boundary, north boundary, south boundary).

3.3.5 Validation of Data

Calibration and validation of the model are the most important requirement for any numerical model study. This can be achieved by the level of confidence in the prediction of models and best possible accuracy after calibration for properly optimized. First approach the performance of the models can be evaluated by calculating the statistical parameters like a correlation coefficient, RMAE, and Index of agreement from the model simulation [28]. Further, quantifying the validation process, three skill tools, i.e., the correlation coefficient (γ), relative mean absolute error (RMAE), and index of agreement (IoAd) are applied for the entire simulation period as per equation mentioned below, respectively. The equation for the correlation is

$$\gamma = \frac{\sum (Q_m - \overline{Q_m})(Q_c - \overline{Q_c})}{\sqrt{\sum (Q_m - \overline{Q_m})^2 (Q_c - \overline{Q_c})^2}}$$

where Q_m and Q_c are the measured value and computed value, respectively, and $\overline{Q_m}$ and $\overline{Q_c}$ are the measured mean value and computed mean value.

RMAE is very vital for comparison of time series data on water level elevation and current velocities since it accounts for both the magnitude and direction of the flow. The RMAE has been used by several authors [29, 30] to evaluate the numerical model result and is defined by Walstra et al. [31] as

$$RMAE = \frac{(|Q_m - Q_c|)}{(|Q_m|)}$$

Though the experience with RMAE parameter is limited (Table 2).

The IoAd, another important tool for quantifying the performance of the model [32, 33], is given by

$$IoAD = 1 - \frac{\sum_{i=1}^{n} (Q_m - Q_c)^2}{\sum_{i=1}^{n} (|Q_c - \overline{Q_m}| + |Q_m - \overline{Q_m}|)^2}$$

Table 2 Classification of error ranges for RMAE

Classification	RMAE
Excellent	<0.2
Good	0.2–0.4
Reasonable/Fair	0.4–0.7
Poor	0.7–1.0
Bad	>1.0

The results are best when IoAd is close to 1 and worst when IoAd is close to 0.

4 Result and Discussion

4.1 Bathymetry

In order to manage the marine environment or to mitigate hazards such as tsunamis or the consequences of climate change, bathymetry plays an important role for the administrations of coastal states. Including bay region, Kakinada coast, ranges in depth from 1.5 to 23.36 m, with the mean depth of 5.79 m are shown in Fig. 2. Kakinada coastline covers a 29 km and its morphology includes a Kakinada bay, Coringa mangrove forest, Hope Island, fishing harbor, deep water port and Kakinada canal (Fig. 1). Like many other bays, near the mouth it is shallow water. The southern half is too shallow and depths never exceed 2 m even in spring tides, while its northern half is 5–13 m deep. This result indicates extensive low-lying areas of Coringa mangrove due to continuous sediment deposition from Godavari channels.

4.2 Hydrodynamic Model

Hydrodynamic modeling is a prerequisite to the spectral wave modeling as it influences the sediment erosion and deposition processes in the coastal region. The present modeling study was carried out to understand the tidal currents and the effect of winds on the current system for the study area. The tidal range of Kakinada coast with a maximum of 2.48 m, which normally occurs at mouth bay in December (NE monsoon), and the minimum level 0.16 m occurs on July 2009. The observed surface elevation is 1.81 m and 2.48 m during SW and NE monsoon respectively (Table 3). Further, the tidal signals are analyzed for major tidal constituents using the IOS method as described by Godin [34] and Foreman [35]. The largest amplitude is observed in M2 constituent in the order of 0.48 and 0.52, which is followed by S2 with 0.18 and 0.21, respectively for SW and NE monsoon. The Greenwich phase of the tidal constituents is 65°–85° for M_2, 106°–340° for S_2, 255°–330° for K_1 and 230°–320° for O_1 during

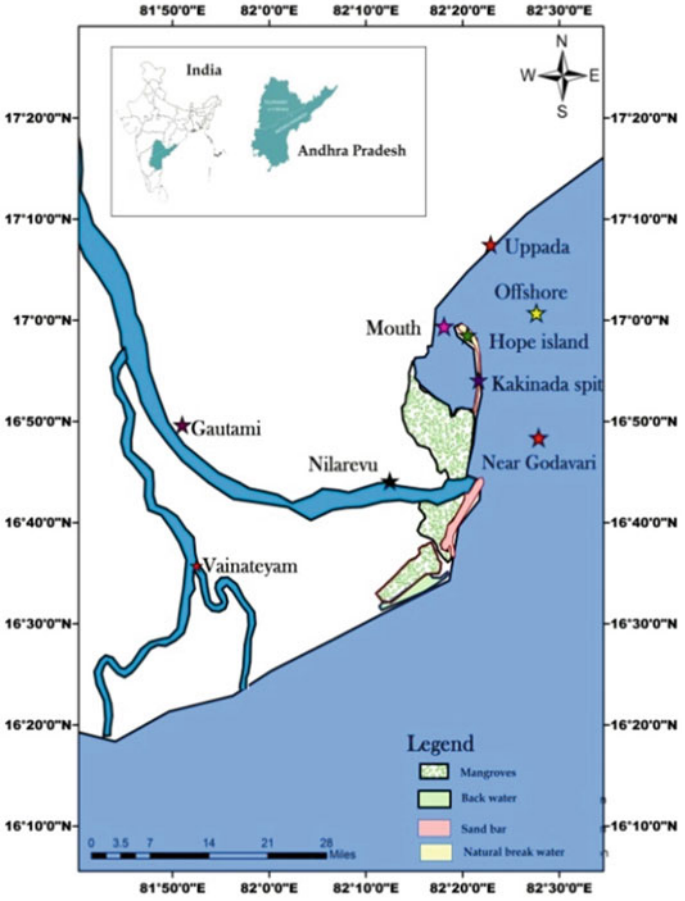

Fig. 1 Study area and sampling locations for Kakinada coast

both seasons. The determined constituents amplitude and phase are given in Tables 4 and 5. The importance of semidiurnal constituent depends on geographical positions which can be calculated by form number. The form number is the ratio of the sums of amplitudes of the two major diurnal (K_1 and O_1) and semidiurnal (M_2 and S_2) constituents [36]. The obtained form numbers are 0.25 and 0.23 during SW and NE monsoon, indicating the study area is dominated by semidiurnal tidal constituents throughout the year.

Tidal currents are very prominent towards the coastal region. Tidal current has been resolved into U components (east–west) and V components (north–south) to get the dominant flow for the coastal environment, which is responsible for sediment transport along or across the coast. Hence, the east of India experiences 0.20–0.25 m/s for coastal current patterns with seasonal changes in direction. Analysis of the current

Table 3 Hydrodynamic parameter during North-east and Southwest monsoon

Location name		Tide (m)			U Velocity (m/s)			V Velocity (m/s)		
		Max	Min	Mean	Max	Min	Mean	Max	Min	Mean
SW	Offshore	1.81	0.17	0.86	0.10	–0.08	0.005	0.23	–0.22	0.013
	Mouth of bay	1.75	0.23	0.86	0.12	–0.13	–0.015	0.13	–0.12	0.018
Monsoon	Near Godavari	1.68	0.19	0.87	0.27	–0.29	–0.012	0.30	–0.15	0.06
	Offshore	1.52	0.18	0.86	0.19	–0.07	0.03	0.22	–0.10	0.03
NE	Mouth of bay	2.48	0.19	0.87	0.21	–0.12	–0.13	0.12	–0.01	0.05
Monsoon	Near Godavari	1.65	0.16	0.87	0.23	–0.27	–0.006	0.15	–0.05	0.03

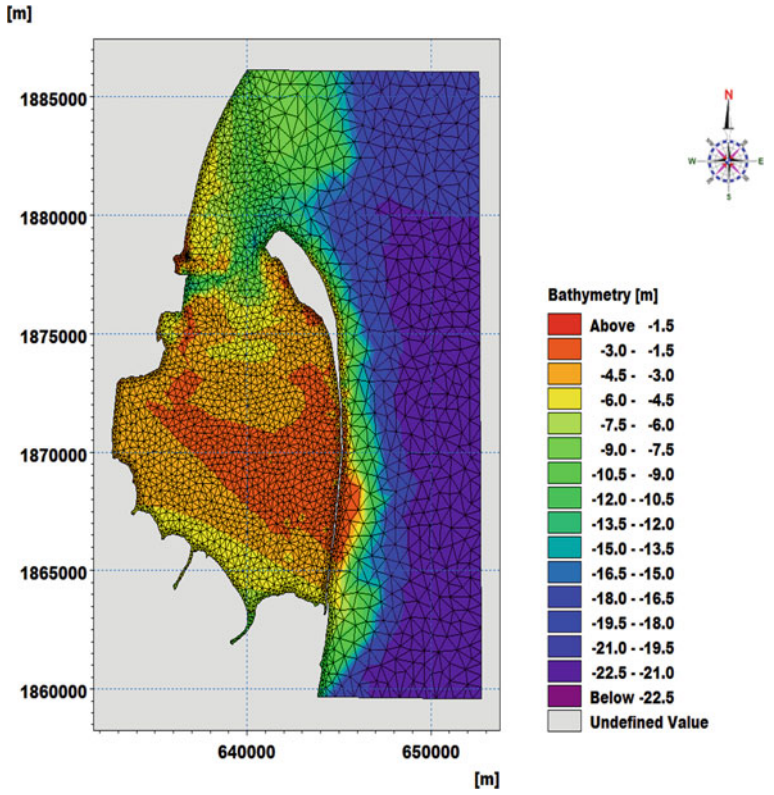

Fig. 2 Mesh with interpolated bathymetry and contour map off Kakinada coast

Table 4 Amplitude of major tidal constituents at various locations

Constituent	M_2, Amplitude (m)		S_2, Amplitude (m)		K_1, Amplitude (m)		O_1, Amplitude (m)	
Locations	Jul-09	Dec-09	Jul-09	Dec-09	Jul-09	Dec-09	Jul-09	Dec-09
1	0.48	0.5	0.18	0.2	0.12	0.13	0.04	0.05
2	0.49	0.52	0.18	0.21	0.13	0.12	0.04	0.05
3	0.48	0.51	0.19	0.21	0.12	0.13	0.04	0.05

speed and direction at measured locations during SW and NE monsoon are given in Table 6. The maximum current speed varied with an average of 0.85 m/s, as 0.88 m/s near Godavari estuary during the NE monsoon. The magnitudes of current speed during the SW monsoon are observed to be higher compared to NE monsoon.

Sastry et al. [4] has revealed that tidal range is less near Godavari estuarine region, and supply of tidal current from the south is strong with relatively larger barrier systems. The flood current reaches maximum velocity and flows in a southerly direction near Kakinada entrance channel and ebb current reaches maximum velocity at

Table 5 Phase of major tidal constituents at various locations

Constituent	M_2, Phase (Deg)		S_2, Phase (Deg)		K_1, Phase (Deg)		O_1, Phase (Deg)	
Locations	Jul-09	Dec-09	Jul-09	Dec-09	Jul-09	Dec-09	Jul-09	Dec-09
1	65	71	119	111	256	328	234	228
2	66	82	127	120	257	297	243	257
3	79	85	138	106	262	319	250	320

Table 6 Observed current magnitude and direction at measured locations

Location	SW monsoon			NE monsoon		
	Average (m/s)	Maximum (m/s)	Direction (Deg)	Average (m/s)	Maximum (m/s)	Direction (Deg)
1	0.21	0.5	NNE	0.12	0.51	SSW
2	0.13	0.72	NNE	0.21	0.54	SSW
3	0.26	0.88	NNE	0.27	0.85	SSW

Godavari point in northern direction that flows along the sand spit (Fig. 3). Since tidal currents were weak and therefore an eroded material tends to be deposited at the mouth entrance and strong ebb current removes materials and has caused deepening of bay. The water level data are predicted using harmonic constituents, which indicate that these oscillations are associated with the semidiurnal pattern. The measured results are compared with modeled U–V components (Fig. 4), which shows that the current in the upper layer increases significantly under the influence of monsoonal winds [37].

4.3 Spectral Wave Model

In coastal engineering, wave hindcast and prediction are important studies for coastal infrastructure development and management. For almost all marine-related activities, knowledge of coastal parameters is very essential. Wave measurement has been carried out from 14th to 29th July and 15th to 30th December 2009, which is considered as southwest (SW) and northeast (NE) monsoon as shown in Table 7. During the study period, the measured wave directions are predominantly from southeast to south for SW and northeast to southeast for NE (Fig. 5a, b). For wave generation, a wind plays a crucial role by varying in heights and periods while moving in different directions. During this period the wind direction is in the range 117° (SW) and 39° (NE) true north (Fig. 6a, b) and maximum wind speeds up to approximately 6.1 m/s (SW) and 4.4 m/s (NE).

For estimating the nearshore wave parameter, the use of numerical models would be helpful to understand the wave effects along coastal regions by testing different wave conditions. The model results are given from the study carried out at Kakinada

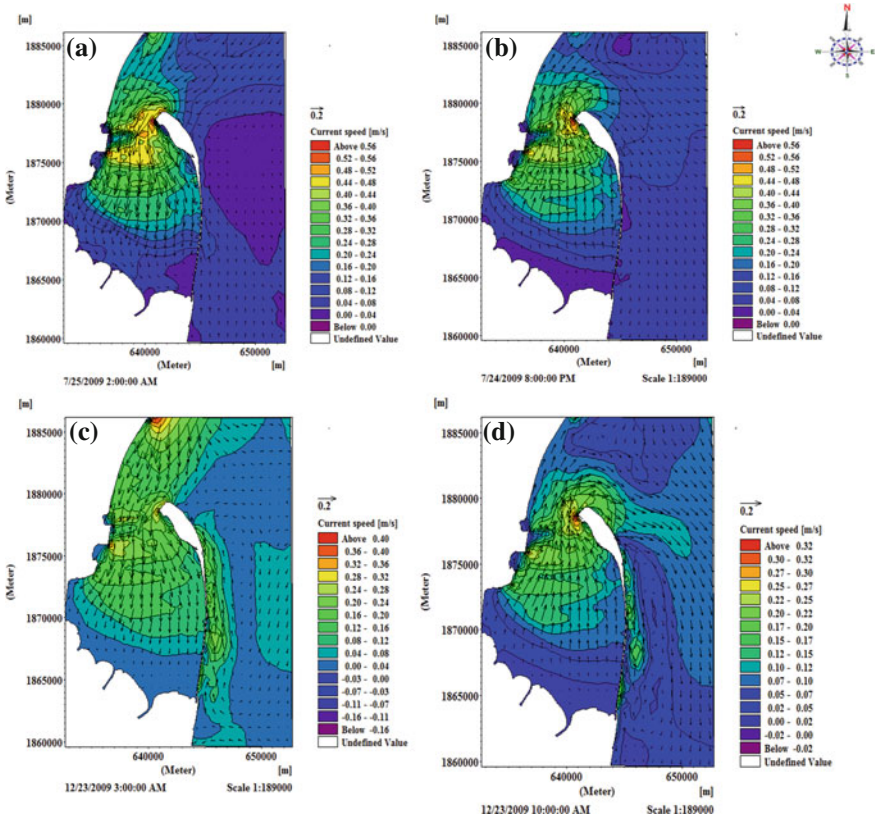

Fig. 3 A flow of current during flood tide and Ebb tide for NE monsoon (**a** and **b**) and SW monsoon (**c** and **d**)

Coast during northeast and southwest monsoon. The study area is typical in its complex bathymetry, where the offshore waves penetrate around the offshore island (Hope Island) in which wave diffraction and refraction effects are considerable. Model calculation reveals that wave height for the offshore region varies as 1.02 m for SW and 1.04 m for NE monsoon as shown in Fig. 7. While the waves reach the Hope Island, the waves get diffracted, refracted and enter into the bay region. The waves reach up to 2 km from the mouth with reduction in wave height of 0.2 m. At a particular time step, the waves approaching the coast has the average value of wave heights 0.75 m with a peak period of 9.24 s. These waves are short in nature and mainly wind-generated waves. Figure 8 shows the comparison between the simulated and observed time series wave parameters.

For generation of these currents, the principle mechanisms are the momentum flux gradients (radiation stress [38]) and it is owed to the decay of the incident waves. Further, simulation results show that the wave radiation stresses reach a maximum of 0.87 m^3/s^2 (SW) and 0.52 m^3/s^2 (NE) along the coast, while 0.62 m^3/s^2 (SW) and

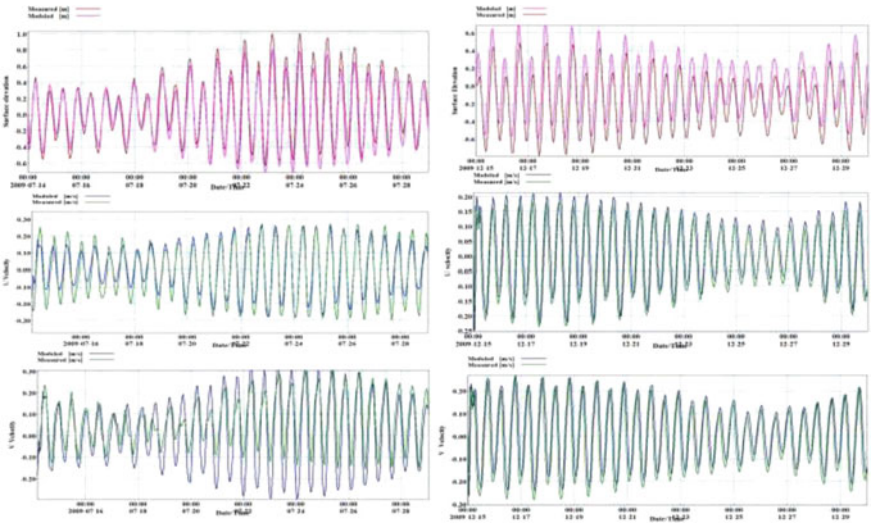

Fig. 4 Comparison of surface elevation U velocity and V velocity between modeled and measured for southwest and northeast monsoon at north-near the bay mouth

Table 7 Wind and wave parameter for north-east and southwest monsoon

Parameter	SW monsoon			NE monsoon		
	Min	Max	Mean	Min	Max	Mean
Significant wave height (Hs) (m)	0.34	1.19	0.67	0.31	0.89	0.54
Mean period (Tm) (s)	6.9	12.6	9.5	4.8	9.4	7
Peak period (Tp) (s)	6.7	18.2	11.3	4.7	14.2	8.1
Zero up crossing period (Tz) (s)	6.31	12.06	8.99	4.46	8.79	6.72
Mean direction (Deg)	92	232	151	67	224	118
Wind speed (U) (m/s)	0.4	6.1	2.61	0.1	4.4	1.53
Wind direction (Deg)	98	145	117.1	0.2	117.5	39.79

0.52 m^3/s^2 (NE) are perpendiculars to the coast. Shear radiation stresses are quite less as the waves approach the coast almost perpendicularly with an average value of S_{xy} as 0.06 (0.08) m^3/s^2 for southwest (northeast) monsoon.

Along Andhra coast, the waves approach from a southerly to southeasterly direction during March to September and northeasterly to east–southeasterly direction for the remaining period [4]. An examination of the wave model shows that the waves

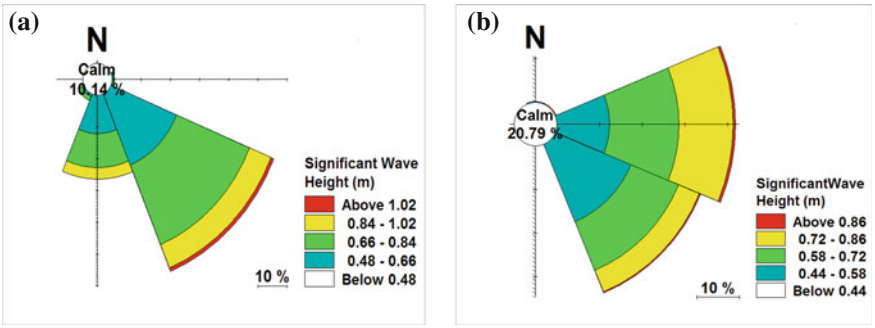

Fig. 5 Wave rose plots for significant wave height at offshore boundary during **a** SW and **b** NE monsoon

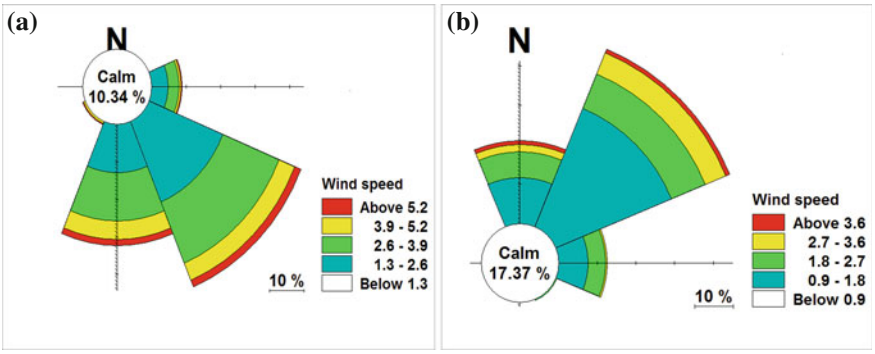

Fig. 6 Wind rose plots for wind speed during **a** SW and **b** NE monsoon

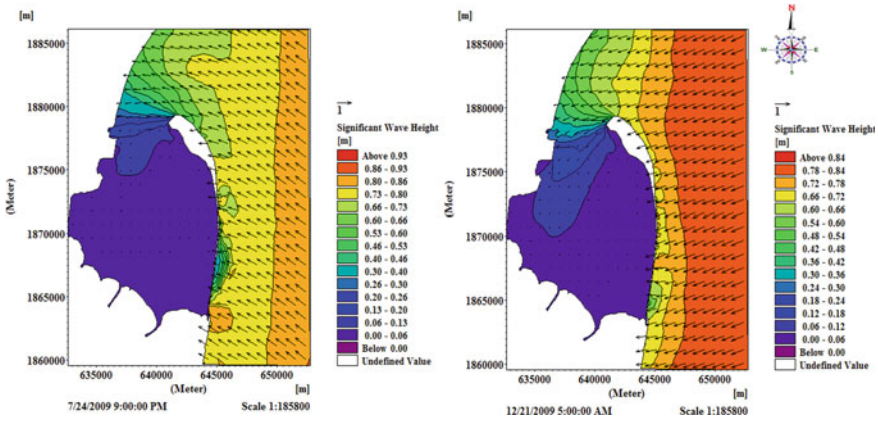

Fig. 7 Simulation of significant wave height with wave direction during SW and NE monsoon

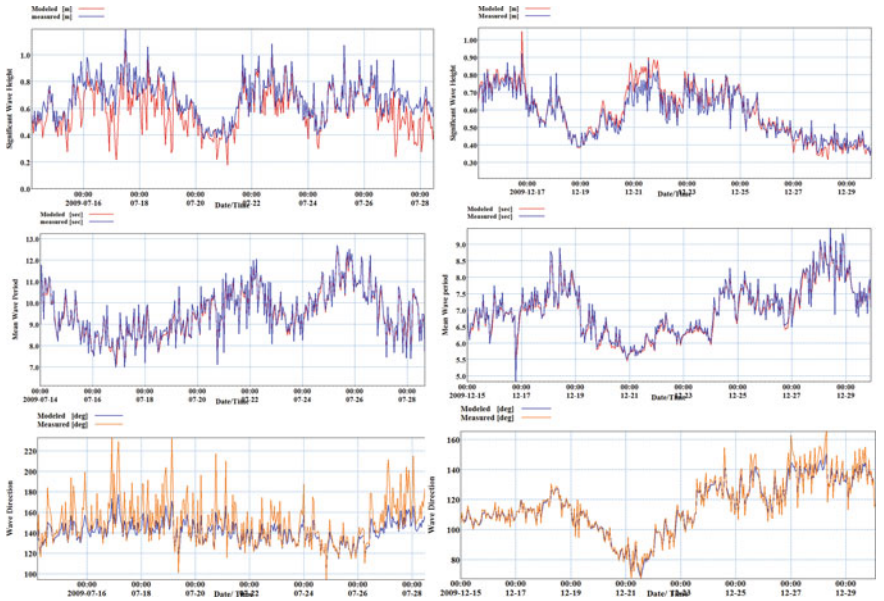

Fig. 8 Comparison between modeled and measured significant wave height, mean wave period and mean wave direction at south near Godavari estuary(c) during SW and NE monsoon

approaching this part of the coastline from South to Southeast and East to Southeast during SW and NE monsoon. The calculated wave parameters are characterized by mean wave period (Tm) with an average of 9.5 (7.0) and significant wave heights (Hs) below 1.2 (0.9) m for SW (NE) monsoon. The relatively higher values of the wave period and significant wave height are related with the relatively stronger winds blowing over a longer fetch distance [39]. The inner portion of Kakinada bay forms a wave, shadow zone from waves coming from the NE and SW monsoon. The overall result indicates that near the mouth of Kakinada bay and north of Godavari estuary are wave converging points, while at the interior of the bay region, waves get diverged. Because of the convergence of wave energy near the entrance of the bay, removal of sediments especially lighter materials takes place. This coincides with the presence of sandy materials up to 2 km from the mouth. In the most interior part of the bay, wave rays are diverged indicating the reduction of wave activity and consequent deposition of clay and silt materials. These results agree well with the observations of Gujar et al. [40], Chevalier et al. [41]. It can also be seen that the occurrence of deviation is more in SW monsoon than NE monsoon season. This might be the reason for changes in wind sea dominant during the SW monsoon [42].

A change in the momentum flux (Radiation stress) is caused by the waves that affect the mean motion of water and its level. Radiation stresses are responsible for the setup and set down of longshore current in the nearshore region. Cross-shore currents are created due to the normal radiation stress (S_{xx} and S_{yy}) and longshore currents

are created due to the shear radiation stress (S_{xy} and S_{yx}) in the water column. In the nearshore region, the total shear stress depends upon the three parameters such as currents, waves, and water level modulation. Particularly, wave shear stress is stronger near the coast (5 km), reaches 1 N m^{-2} as the reference wave, but there is a rapidly decreases of its intensity with bathymetry and vanishes 20 km offshore [41]. The total shear stress varies with time as current and wave action on the bottom along with the tidal cycle. The wave shear stress enhances at low tide for smaller depth and while current shear stress evolves with minimal currents, i.e., maximum at ebb tide due to combination of tidal currents. Therefore, at the entrance of the bay total shear stress is maximum at low tide and minimum of flood tide. Moreover, the incidence angle of wave affects directly the convergence and divergence of wave around the coastal area; as a result, erosion and deposition are certainly modulated by ordination of wave [41].

4.4 Validation of Model

For all modeler opinions, simulations depend on data availability, characteristics of the water body, model calibration, and validation process [43]. Comparison of the models computed with measured data provides the gross confidence in the performance. To perform the model validation, the model is run during two monsoons in which various tunning parameters are changed. These above model validations have been compared to all three stations with the time series data collected at SW and NE monsoon, respectively. The three skills tests are performed to quantify the model performance with observed data for both monsoons separately. The values of the correlation coefficient, RMAE and IoAd are shown in Tables 8 and 9. It provides a good confidence in model validation for all the wave and current parameters.

4.5 Sediment Transport

Knowledge on the process of sediment transport remains as a large gap for continuous development and well-validated practical modeling system. Hence analyses on longshore sediment transport were carried along the Kakinada coast for SW and NE monsoon.

With the information on waves available over the two-dimensional model, the hydrodynamic model calculates the wave forcing corresponding to the simulated coastal current. Finally, waves and current information are passed to sediment transport module to calculate the sediment dynamics for both SW and NE monsoon. Along the east coast of India, especially in the Kakinada bay circulations are controlled by the coastal current. The coastal current changes its direction seasonally, being northerly from January to July and southerly from August to December. The direction of current during this period is between southeast and southwest. These

Table 8 Correlation coefficient, RMAE, and IoAd at Kakinada coast obtained from measured and modeled parameter for SW monsoon

Parameters	SW monsoon								
	Correlation coefficient			RMAE			IoAd		
Location	1	2	3	1	2	3	1	2	3
Surface elevation	0.86	0.93	0.89	0.05	0.08	0.02	0.90	0.96	0.94
Current U component	0.80	0.93	0.76	0.25	0.19	0.20	0.91	0.90	0.95
Current V component	0.78	0.90	0.92	0.33	0.23	0.19	0.90	0.91	0.96
Significant wave height	0.85	0.91	0.73	0.10	0.80	0.10	0.93	0.97	0.84
Mean wave period	0.60	0.79	0.84	0.08	0.10	0.08	0.78	0.6	0.74
Mean wave direction	0.82	0.90	0.87	0.09	0.20	0.08	0.90	0.88	0.83

Table 9 Correlation coefficient, RMAE, and IoAd at Kakinada coast obtained from measured and modeled parameter for NE monsoon

Parameters	NE monsoon								
	Correlation coefficient			RMAE			IoAd		
Location	1	2	3	1	2	3	1	2	3
Surface elevation	0.84	0.78	0.93	0.12	0.15	0.03	0.92	0.86	0.81
Current U component	0.94	0.75	0.92	0.24	0.35	0.21	0.91	0.84	0.89
Current V component	0.91	0.64	0.90	0.33	0.26	0.30	0.85	0.81	0.85
Significant wave height	0.81	0.76	0.92	0.10	0.20	0.10	0.92	0.86	0.96
Mean wave period	0.84	0.75	0.71	0.20	0.20	0.20	0.52	0.65	0.45
Mean wave direction	0.82	0.71	0.89	0.04	0.1	0.04	0.95	0.61	0.96

currents do not seem to be influenced much by the tides [4]. Wave refraction studied by Sastry [44] indicates that when the direction of wave is southeast, the associated littoral current is directed toward upcoast while it is directed toward downcoast for the waves approaching in a northeasterly direction. During the study period, the longshore current is predominantly directed to the north for SW and NE monsoon. This is due to the wave heights and littoral current of southwest monsoon season are higher and stronger than those of the northeast monsoon season which results in a net northerly drift all along the Kakinada coast. It is observed that for waves approaching the coast from southeast, the longshore current is toward the north. This result suggests that the sediments in the nearshore region get transported from south of the Kakinada spit to toward; the north of the Hope Island deflects toward the Uppada region and tends to erode in this region.

The coupled model computes hydrodynamic parameters as well as rates of sediment direction and finally calculated the bed-level change within the model. The erosion and deposition rates refer only to the changes of initial bed level which are predicted by the model. On observation, the bed level change rates would be much smaller as the initial bed level change and decreases quickly due to resultant change in the bathymetry [45]. The faster bed change is associated with the smaller morphological time steps and vice versa [46]. The absolute value of the rate of bed-level change is calculated for the whole domain which concludes that the change in bed level is prominent over the entrance of the bay during the SW monsoon than NE monsoon which is due to nearshore dynamics. Thus, bed-level change is used to update the nearshore topography which in turn simulates the realistic factors affecting coastal morphology. This study shows that for both SW and NE monsoon the northern part of Godavari estuary is getting eroded while deposition is occurring near the mouth of Kakinada bay region. However, the rate of bed level change is lesser in NE monsoon than the SW monsoon near the mouth of Kakinada bay. Therefore, throughout the study period, bed-level changes show higher rate during the SW monsoon along the Kakinada coast (Fig. 9).

In the inner portion of nearshore or surf zone, the longshore sediment transport is essential due to waves action [47]. In this chapter, simulation shows that the longshore transport is toward the northern direction for waves from the SSE and S, while toward southern direction for waves from NE and ENE direction. This result shows a significant area of deposition along the mouth of the Kakinada bay and around Hope Island. The waves from the southern direction carry sediment along the shoreline from the south (north of Godavari estuary), which is deflected by offshore waves and refracted by the morphological features of Hope Island and deposits in the mouth region of Kakinada bay. The longshore current which is generated by broken waves approaches the coast at different angles. The strength and direction of currents vary with the orientation of local coastline. For improving the navigation, the prediction of wave-induced longshore currents and the sediment transport in the vicinity of ports is important. Longshore sediment transport shows the direction of south to north during SW monsoon and reverse during the NE monsoon (Figs. 10 and 11). Vector shows total load transport over a tidal cycle with the magnitude indicating

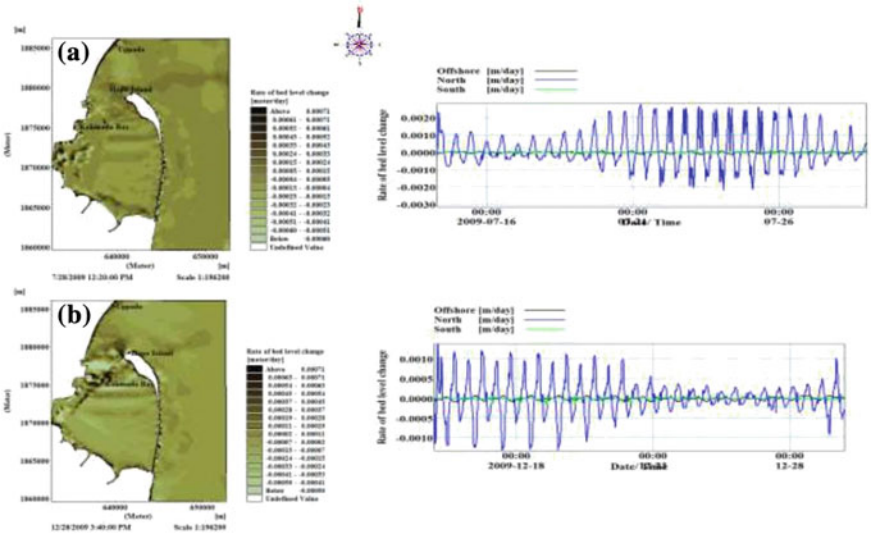

Fig. 9 Initial bed level changes during **a** SW and **b** NE monsoon

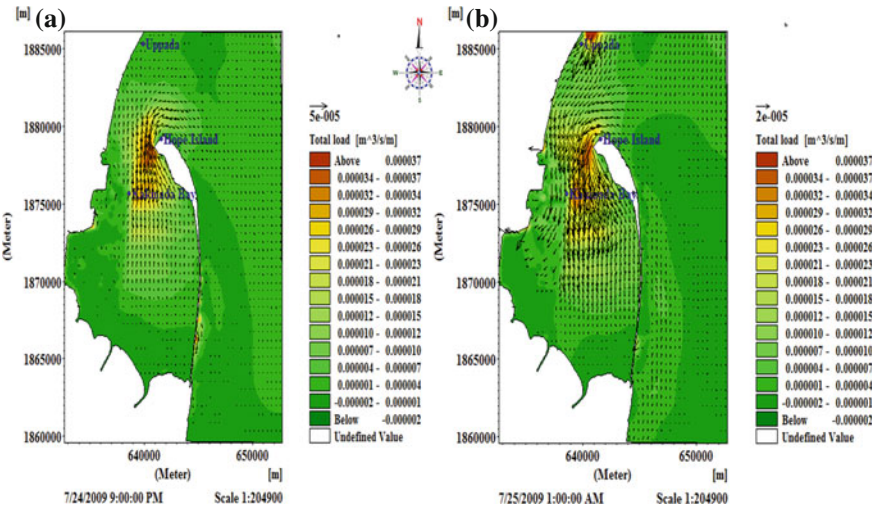

Fig. 10 Simulation of sediment transport with current direction for **a** ebb flow and **b** flood flow during SW monsoon

the amount of sediment transport. This can be attributed to the current direction in this region and confirms with the earlier studies [12].

The coastal engineering Manual [48] states that over the longest possible time period sediment transport rates must be determined. Despite the lack of wave data for our study area, the results are expanded to make rough estimates of annual sedi-

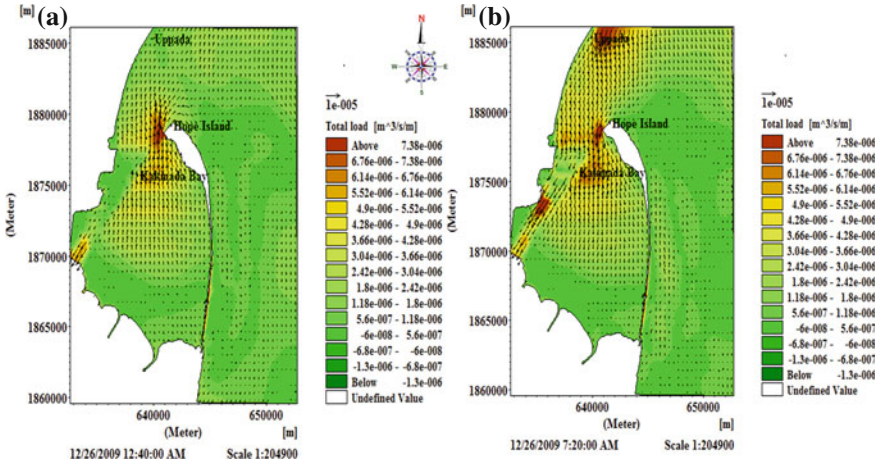

Fig. 11 Simulation of sediment transport with current direction for **a** ebb flow and **b** flood flow during NE monsoon

ment movement, which falls within one order of the current magnitude. In this study, characteristics of sediment transport have been calculated using a 2D model (sediment transport model). The surf zone of Kakinada coast has enormous quantities of sand stir along the shore due to the wave's action with northerly direction for SW and NE monsoon. Chandramohan et al. [49] suggests that along the Andhra coast the predominant direction of sediment transport is toward the northeast from March to October and toward SW during the rest of the year. Sastry et al. [4] has shown that the net transport of sediment along Kakinada coast is toward north, sufficient quantity moves offshore and results in the formation of offshore bars, islands or sand spits.

The rate of sediment transport is very large during the southwest monsoon owing to the prevalence of the high wave climate in the Bay of Bengal. The field measurement of net sediment transport study for Kakinada Coast estimates 0.4×10^3 m^3/year for SW monsoon and 1.2×10^3 m^3/year for NE monsoon which was low due to some error field data. In this paper, the transport is taken from modeled data, which estimates 3.2×10^3 m^3/year for SW monsoon and 7.7×10^3 m^3/year for NE monsoon. The above results nearly coincide with previous research which is estimated as 2.62×10^3 m^3/year along southern longshore sediment transport from October to February and 9.60×10^3 m^3/year along northern transport from March to September with a net drift toward the north [50, 51]. The study on the net sediment transport rate using the energy flux method has northern direction for Indian Coast reported as 0.52 million m^3/year for Visakhapatnam coast [52]. Sarma and Reddy (1988) estimated the net littoral drift of 0.54 million m^3/year toward the northern part of Visakhapatnam. Recently, the report from NSDRC, 2003, shows a transport rate for the Visakhapatnam coast has 0.31 million m^3/year (Southerly) and 0.84 million m^3/year (Northerly). Also, Parchure, 1978 estimates that the net northward littoral

drifts at the Visakhapatnam port as 0.7 million m^3/year. Panigarhi et al. [47] has conceded a theoretical estimation and he reported that the gross sediment transport varied between 1.12 and 1.64 million m^3/year and the net sediment transport varied between 0.5 and 0.7 million m^3/year. From the above study, the quantity of long-shore sediment transport rate increases from Godavari estuary up to the mouth of Kakinada bay and then gradually decrease in Uppada region indicating maximum sediment transport within the mouth region.

5 Summary and Conclusion

Prediction of morphological changes has immense application for development of coastal infrastructure. More relevantly, coastal erosion has major problems faced by several sectors which needs to develop the model for the concern coasts. An investigation is done on numerical modeling of morphological changes by dynamic coupling of waves and currents using MIKE 21 Flexible mesh coupled model. The main objective of the research is to simulate hydrodynamic, spectral and sediment transport model and are compared with corresponding observed data for which field data collected for SW and NE monsoon 2009 and processed.

From the processed data, the tide ranges with a maximum of 2.48 m normally occurred at mouth bay in December (NE monsoon), and the minimum level of 0.16 m occurred in July. The observed surface elevation was 1.81 and 2.48 m and obtained form number was 0.25 and 0.23 during SW and NE monsoon. This indicates that Kakinada coast has dominance of semidiurnal tidal constituents throughout the year. The highest current speed was about 0.88 (0.85) m/s at north of Godavari estuary (location 3), which was followed by the mouth of Kakinada bay about 0.72 (0.54) m/s during SW (NE) monsoon. The measured wave directions were predominantly from southeast to south for SW monsoon and north to northeast for NE monsoon. The model calculation reveals that the wave height of the offshore region varied as 1.04 m for NE and 1.02 m for SW monsoon. At a particular time step, the waves approaching the coast the average value of wave heights is 0.75 m with a peak period of 9.24 s. The overall results indicated the flood current reached maximum in southern direction near the entrance channel and ebb current reached maximum at Godavari point, flows in northern direction along the sand spit. Near the mouth of Kakinada bay and north of Godavari estuary, the waves had converging points, while at the interior of the bay region the waves got diverged. Due to convergence of wave energy near the entrance bay, there was removal of sediments especially lighter sediments. This was coincides with the presence of sandy materials up to 2 km from the mouth of bay. In the most interior part of the bay, the wave rays diverge with reduction in wave activities and consequently deposition of clay and silt materials occurs. It could also be seen that the occurrence of deviation was more in SW than in NE monsoon. This might be the reason for changes in dominant of wind sea during SW monsoon and the current in the upper layer increased significantly under the influence of monsoonal winds.

Further, simulation results show that the wave radiation stresses reach a maximum of 0.87 m^3/s^2 (SW) and 0.52 m^3/s^2 (NE) along the coast, while 0.62 m^3/s^2 (SW) and 0.52 m^3/s^2 (NE) are perpendiculars to the coast. Therefore, in this model, the domination of wave shear stress occurs near the entrance of the bay and current domination toward offshore. At the entrance of the bay, total shear stress is maximum at low tide and minimum of flood tide. Moreover, the incidence angle of wave affects directly the convergence and divergence of wave around the coastal area; as a result, erosion and deposition are certainly modulated by ordination of wave.

The calibration was made against three stations at Kakinada coast during south-east and northwest monsoon. In the calibration process scattering index was reduced to obtain best results, it was made through several runs by changing various tuning parameters. Overall comparisons and validation between modeled data with measured data showed that the models were in good correlation with similar quantities of the measured data.

Initial bed change plays a vital role in prediction of erosion and deposition. Simulated bed level change rate showed that the area north of Godavari estuary was getting eroded while near the mouth of Kakinada bay was getting deposited for both SW and NE monsoon. However, the rate of bed level change was lesser near the mouth of Kakinada bay in NE monsoon than the SW monsoon. Therefore, throughout the study period, change in bed level showed higher rate during the SW monsoon along the Kakinada coast. Simulation shows that the longshore transport is toward northern direction for waves from the SSE and S, while toward southern direction for waves from NE and ENE direction This result showed a significant area of deposition was noticed along the mouth of the Kakinada bay and around Hope Island. The waves from the southern direction carried sediment along the shoreline from the south (north of Godavari estuary), deflected by offshore waves and refracted by Hope Island and deposits in the mouth region of Kakinada bay. This result suggested that the nearshore sediments were transported from south of Kakinada spit toward the north of the Hope Island and deflected toward the Uppada region where erosion tends to occur.

The net sediment transport was estimated as 3.2×10^3 m^3/year for SW monsoon and 7.7×10^3 m^3/year for NE monsoon, both were present at mouth of Kakinada bay and north of Godavari estuary, respectively. It was understood that the quantity of transport rate was increased from Godavari estuary up to mouth of Kakinada bay, and then gradually decreased to Uppada region, indicating maximum sediment transport occurs within the mouth region. Based on the hydrodynamic data, the modeling of sediment transport results had shown that sediment transport was strongly influenced by wave direction, which significantly enhanced bed shear stress, results in increasing of sediment remobilization. From the above simulation, a large quantity of sediment was carried by rivers and deposited along the mouth of estuary which was piled up into barrier features by the influence of waves. These barrier features are development to form spits along the shoreline, due to the strong longshore drift. The present study shows that instantaneous response in morphological changes by hydrodynamic processes which requires the redistribution of sediment. There is a lag in the morphological response to hydrodynamic forcing which is considered as

a time-dependent coupling mechanism, this is due to time management of sediment from one region to another. Hence morphodynamic processes disclose the positive and negative feedbacks toward shoreline region of Kakinada coast which results in the designing, constructing and maintaining of coastal and maritime projects.

6 Future Recommendation

The present study has been very useful to understand the dynamics of coastal landforms such as beaches, shorelines, and sand spits, etc. Even though it helps in elucidating the information on landform features and the related coastal processes, the study could lead to further research and development in the following aspects. For accurate prediction of coastal zone management along Kakinada coast, it is required to collect the in situ continuous hydrodynamic data like wave, tide and current for at least one complete year. Further to validate the modeled data, the sediment trap measurements are to be carried out. The change in coastal landform features will be monitored by undertaking RTK–GPS survey of the coast along with shallow water bathymetry one can estimate the level of erosion and accretion of sediments, in turn, forms sand spits along the Kakinada coast. The above studies further enhance the understanding of coastal land reforms and is useful for coastal infrastructure development and management.

Acknowledgements This study was carried at framework of the MoES research project entitled "Oil Spill Modelling" (Project no: MoES/8-PC/2(2)/2007-PC-IV Dated 27.03.2008) New Delhi. The authors wish to thank Dr. K. Kathirasan, Director and Dean, Faculty of Marine Sciences, Annamalai University, Parangipettai, and Dr. B. R. Subramanian, ICMAM-Project Directorate for his constant encouragement, support and providing all necessary facilities for carrying out this work. Authors also wish to thank all those in the "Oil Spill team" for their valuable support during the field campaign.

References

1. Cowell PJ, Thom BG (1994) Morphodynamics of coastal evolution. In: Crater RWG, Woodroffe CD (eds) Coastal evolution. Cambridge University press, Cambridge, pp 33–86
2. Sambasiva Rao M, Vaidyanadhan R (1979) Morphology and evolution of Godavari delta, Zeitschr. Geomorphology 23(1):243–255
3. Sambasiva Rao M, Vaidyanadhan R (1979) New coastal landforms at the confluence of Godavari river. Indian J Earth Sci 6:222–227
4. Sastry JS, Vethamony P, Swamy GN (1991) Morphological changes at Godavari delta region due to waves, currents and associated physical processes. In Quaternary Deltas of India (ed. Vaidyanadhan, R.). Geol Surv India 22:139–151
5. Rengamannar V, Pradhan PK (1991) Geomorphology and evolution of Godavari delta. In Quaternary Deltas of India (ed. Vaidyanadhan, R.). J Geol Soc India 22:51–64
6. Ramakumar M (2000) Recent changes in Kakinada Spit, Godavari Delta. J Geol Soc India 55:183–188

7. Ramkumar M (2003) Progradation of the Godavari delta—a fact or empirical artifice? insights from coastal landforms. J Geol Soc India 62:290–304
8. Reddy NPC, Mohan Rao K (1996) Sedimentological and clay mineral studies in Kakinada Bay, east coast of India. Indian J Geomar Sci 25:12–15
9. Reddy NPC, Rao BP, Rao KM, Rao VS (1994) Seasonal changes in suspended sediment load in the Gauthami-Godavari estuary. Mahasagar-Bull Natl Inst Oceanogr 27(1):47–53
10. Harsha sundar E, Reddy KSN, Vani Sailaja V, Murthy KNVV (2010) Textural characteristics of coastal sands between Kakinada bay and Tandava river confluence Andhra Pradesh, East coast of India, J Indian Assos Sedimentol 29(1):61–69
11. Murty PS, Pandey Ashish, Suryavanshi Shakti (2014) Application of semi-distributed hydrological model for basin level water balance of the Ken basin of Central India. Hydrol Process 28:4119–4129
12. Raju NSN, Kumar KA, Gowthaman R, Kumar VS, Kumar SJ (2004) Coastal processes along north Kakinada coast, Andhra Pradesh based on short-term study. Technical report: NIO/TR-2/2004. National Institute of Oceanography, India
13. Hema Malini B, Nageswara Rao K (2004) Coastal erosion and habitat loss along the Godavari delta front—a fallout of dam construction. Curr Sci 87:1232–1236
14. Tripathi NK, Rao AM (2001) Investigation of erosion on Hope Island using IRS-1D LISS-III data. Int J Remote Sens 22(5):883–888
15. Padma kumari K, Jnaneswari D, SubbaRao DV, Sridhar P (2012) Applications of remote sensing and geographical information system techniques on Geomorphological mapping of coastal part of East Godavari district, Andhra Pradesh, India. Int J Eng Sci Technol 10(4):4296–4430
16. Padma kumari K, Hasmath jahan, Subba Rao (2012) Applications of remote sensing and GIS techniques for land use/land cover, wetland mapping of coastal part of East Godavari District, Andhra Pradesh, India. Int J Earth Sci Eng 4(6):908–914
17. Padma kumari K, Hasmath jahan, Subba Rao, Sridhar P (2012) Shoreline morphometric change analysis using remote sensing and GIS in the coastal part of East Godavari District, Andhra Pradesh, India. Int J Civil Eng Appl Res 2(3):129–136
18. Padma Kumari K, Killi Srinivas, Gopi Krishna Kasyap V (2015) Shoreline change analysis of erosion and deposition using landsat data 2000 & 2015. In: Proceeding of computer science and electronic engineering conference, The Coastal part of East Godavari District, Andhra Pradesh, India, 2015, pp 111–123
19. Guru Prasad Ch, Gaddem NR (2014) Global warming affects on Fishing village in India (A case study on Andhra coastal village: Uppada). IOSR J Appl Geol Geophys (IOSR-JAGG) 2(2):50–56
20. Nageswara Rao K (2006) Coastal morphodynamics and asymmetric development of the Godavari delta: implications to facies architecture and reservoir heterogeneity. J Geol Soc India 67:609–617
21. Nageswara Rao K, Sadakata N, Hema Malini B, Sarma VVLN, Takayasu K, Kawase M (2003) Reconstruction of the stages in Holocene evolution of Godavari delta, India: a preliminary study. Trans Jpn Geomorphol Union 24:295–309
22. Satyaprasad D (1986) Morphodynamics of the beaches and sand spit, Kakinada Bay, East Coast of India. PhD thesis, Andhra Pradesh, Andhra University
23. Jain S, Sridhar PN, Veera Narayan B, Surendran A (2008) Morphodynamics of Godavari Tidal Inlets. Monit Model Lakes Coast Environ 237–243
24. Sørensen OR, Kofed-Hansen H, Rugbjerg M, Sorensen LS (2004) A third generation spectral wave model using an unstructured finite volume technique. In: Proceeding of 29th international conference on coastal engineering, Lisbon, Portugal
25. Komen GJ, Cavaleri L, Donelan M, Hasselmann K, Hasselmann S, Janssen PAEM (1994) Dynamics and modelling of ocean waves. Cambridge University Press, Cambridge, New York, USA, p 532
26. Geils J, Stoschek O, Matheja A (2001) 4th DHI software conference MIKE 21/MIKE 3 for modeling hydrodynamics in a brackish tidal environment by coastal engineering, pp 1–22

27. Narasimham KA, Selvaraj GSD, Lalitlia Devi S (1984) The Molluscan resources and ecology of Kakinada Bay. Marine Fisheries Information Services, Technical & Extension Series 59:1–16
28. Kankara RS, Mohan R, Venkatachalapathy R (2011) Hydrodynamic modelling of Chennai coast from a coastal zone management perspective. J Coast Res 29(2):347–357
29. Fernandes EHL, Dyer KR, Niencheski LFH (2001) TELEMAC-2D calibration and validation to the hydrodynamics of the Patos Lagoon (Brazil). J Coast Res 34:470–488
30. Sousa MC, Dias JM (2007) Hydrodynamic model calibration for a mesotidal lagoon: the case of Ria de Aveiro (Portugal). J Coast Res (Special Issue 50). In: Proceedings of 9th international coastal symposium, pp 1075–1080, Gold Coast, Australia
31. Walstra DJR, Van Rijn LC, Blogg H, Van Ormondt M, (2001) Evaluation of a hydrodynamic area model based on the COAST3D data at Teignmouth 1999, TR121-EC MAST Project no. MAS3-CT97-0086. HR Wallingford, Oxfordshire, UK
32. Dawson CW, Abrahart RJ, See LM (2007) HydroTest: a web based toolbox of evaluation metrics for the standardised assessment of hydrological forecasts. Environ Model Softw 22:1034–1054
33. Wilmott CJ (1981) On the validation of models. Phys Geogr 2:184–194
34. Godin G (1972) The analysis of tides. University of Toronto press, Toronto
35. Foreman MG (1977) Manual for tidal height analysis and prediction. Pacific Marine Science report 77-10. Instiute of Ocean Sciences, Canada
36. Pugh DT (1987) Tides, surges and mean sea level. Wiley, Chichester, p 472
37. Vethamony P, Babu MT (2010) Physical processes in Gulf of Kuchchh: a review. Indian J Geo-mar Sci 39(4):497–503
38. Longuet Higgins MS, Stewart RW (1964) Radiation stress in water waves a physical discussion with application. Deep Sea Res 11:529–562
39. Poulos SE, Chronis G Th (2001) Coastline changes in relation to longshore sediment transport and human impact, along the shoreline of Kato Achaia (NW Peloponnese, Greece). Mediterr Mar Sci 2(1):5–13
40. Gujar AR, Angusamy N, Rajamanickam GV (2008) Wave refraction patterns and their role in sediment redistribution along South Konkan, Maharashtra, India. Geoacta Int J Earth Sci 7:69–79
41. Chevalier C, Froidefond JM, Devenon JL (2008) Numerical analysis of the combined action of littoral current, tide and waves on the suspended mud transport and on turbid plumes around French Guiana mudbanks. Cont Shelf Res 28(4–5):30, 545–560
42. Remya PG, Kumar R, Basu S, Sarkar A (2012) Wave hindcast experiments in the Indian Ocean using MIKE 21 SW model. J Earth Syst Sci 121(2):385–392
43. Hsu MH, Kuo AY, Kuo JT, Liu WC (1999) Procedure to calibrate and verify numerical models of estuarine hydrodynamics. J Hydraul Eng 125:162–182
44. Sastry JS (1958) Some aspects of shoreline processes and physical oceanography. D.Sc. thesis, Andhra University
45. Mishra P, Pradhan UK, Patra SK, Ramanamurthy MV, Seth B, Mohanthy PK (2014) Field measurements and numerical modeling of nearshore processes at an open coast port the east coast of India. Indian J Geomar Sci 43(7)
46. Saied UM, Tsanis IK (2005) ICEM: integrated coastal engineering model. J Coast Res 21(6):1257–1268
47. Panigrahi JK, Sathish Kumar V, Tripathy JK (2010) Littoral drift by alongshore flow at Visakhapatnam East Coast of India. J Hydro-Environ Res 1–11
48. CERC-Coastal Engineering Research Centre (2003) Coastal engineering manual, Publication EM 1110-2-1100, online Manual for USACE
49. Chandramohan P (1988) Longshore sediment transport model with particular reference to the Indian Coast. Unpubl. PhD thesis, IIT Madras, 210
50. Chandramohan P, Sanil Kumar V, Nayak BU (1991) Wave statistics around Indian Ocean. Indian J Geomar Sci 20:87–92

51. Nayak BU, Chandramohan P, Sakhardande RN (1992) Seasonal distribution of wave heights off Yanam on the east coast of India. J Inst Eng 72:187–193
52. Chandramohan P, Nayak BU (1999) Longshore sediment transport along the Indian Coast. Indian J Geomar Sci 20:110–114

Dr. N. Sharmila received M.Sc., in Ocean Science and Technology from Annamalai University, Tamil Nadu, India, in 2009. Received Ph.D. in Ocean Science and Technology from Annamalai University, Tamil Nadu, India, in 2017. She has published more than four International papers in various reputed journals and also has been acting as a reviewer for various journals. She is actively involved as a member in various professional bodies. Presently working as a Professor and Head in International Maritime Academy, Department of Naval Architecture and Ship Building, Chennai, India. Her current research interest is Numerical modeling—MIKE 21 Coupled (Hydrodynamic, Spectral, Sediment transport) model.